Analysis and Correction of Dual-PRF Velocity Data

Iwan Holleman and Hans Beekhuis,
Royal Netherlands Meteorological Institute (KNMI),
e-mail: holleman@knmi.nl

Submitted to the Journal of Atmospheric and Oceanic Technology (AMS)

Abstract

The dual Pulse Repetition Frequency (dual-PRF) technique for extension of the unambiguous velocity interval is available on many operational Doppler weather radars. Radial velocity data obtained from a C-band Doppler radar running in dual-PRF mode has been analyzed quantitatively. The standard deviation of the velocity estimates and the fraction of dealiasing errors are extracted and related using a simple model. A post-processing algorithm for dual-PRF velocity data, which removes noise and corrects dealiasing errors, has been developed and tested. It is concluded that the algorithm is very efficient and produces high-quality velocity data.

1 Introduction

Doppler weather radars are capable of providing high quality wind data at a high spatial and temporal resolution. This kind of data is of great value for operational weather forecasting and Numerical Weather Prediction (NWP) models. Doppler velocity information can be used for removal of ground clutter, extraction of wind profiles, detection of shear zones, and construction of dual-Doppler wind fields (Meischner et al., 1997; Serafin and Wilson, 2000; Chong et al., 2000). In addition, the wind profiles and radial velocity data can be assimilated into NWP models (Collins, 2001; Lindskog et al., 2000). Operational application of Doppler data from weather radars is hampered, however, by the infamous limitation of the range-velocity ambiguity. This is particularly true for a C-band weather radar, since its ambiguity limitation is a factor of two more stringent than that of an S-band radar. Aliased velocity data from S-band radars can be unfolded using local continuity in one or more dimensions and environmental constraints (Hennington, 1981; Merritt, 1984; Desrochers, 1989; Bergen and Albers, 1988; Eilts and Smith, 1990). Eilts and Smith (1990) have found that velocity data of acceptable quality is obtained for these radars provided that the wind shear is not extreme. Due to the smaller unambiguous velocity interval, this kind of approach is not feasible for C-band radars without relying heavily on external wind profiles (Hondl and Eilts, 1993). To this day, Doppler data from the operational C-band weather radars in Europe is mainly used for removal of ground clutter and extraction of wind profiles (Meischner et al., 1997).

Sirmans et al. (1976) have proposed the use of two interlaced sampling rates for the extension of the unambiguous velocity. The application of this staggered Pulse Repetition Time (PRT) technique is hampered thus far by the inability of most operational weather radars to run in staggered PRT mode and associated problems with filtering of ground clutter. To tackle the latter problem, Sachidananda and Zrnić (2000) have presented a new processing algorithm based on Fourier transform and magnitude deconvolution. Dazhang et al. (1984) have put forward a method wherein velocity estimates are made using two alternating Pulse Repetition Frequencies (PRFs), i.e., employing M_1 pulses at one PRF followed by M_2 pulses at the other PRF. This dual-PRF technique allows for straightforward filtering of ground clutter and an extension of the unambiguous velocity interval. The dual-PRF technique is available on a large part of the operational (C-band) Doppler weather radars, but it is not used widely as of yet. Recently, the interest in the dual-PRF technique for extending the unambiguous velocity interval of C-band and X-band radars has increased. Jorgensen et al. (2000) have reported on the use of the dual-PRF scheme for mitigating velocity ambiguities of an X-band airborne Doppler radar. They present examples of raw radial velocity data from this radar and discuss the cause of the dealiasing errors. The effect of azimuthal shear of the radial wind on the quality of dual-PRF data has been investigated by May (2001) using a mesocyclone model. May and Joe (2001) have presented an algorithm for correcting dealiasing errors in dual-PRF velocity data.

In this article we present an extended analysis of dual-PRF velocity data and a three-step post-processing algorithm for correction of the data. First, a short introduction to the dual-PRF technique and a description of the available Doppler data are given. Then, qualitative and quantitative characteristics of dual-PRF data are elucidated via different analyzes of measured velocity fields. These analyzes confirm that the velocity outliers, which are characteristic for dual-PRF data, are in fact isolated dealiasing errors. Finally, a three-step algorithm for the correction of dual-PRF velocity data is described in detail. The processing algorithm is intended

for operational use, and preliminary results indicate that the quality of the velocity fields is enhanced significantly and that further use of the data has become feasible.

2 Dual-PRF technique

The operational application of Doppler weather radar, especially C-band or shorter wavelengths, has been hampered by the small unambiguous velocity interval of the instrument. The unambiguous or Nyquist velocity of a Doppler radar using uniformly spaced pulses is given by (Doviak and Zrnić, 1993):

$$V_i^u = \frac{\lambda \, \mathrm{PRF}_i}{4} \tag{1}$$

where λ is the wavelength used by the radar and PRF_i is the Pulse Repetition Frequency. The PRF also determines the unambiguous range of the radar. The unambiguous velocity and range of a Doppler radar are coupled, and a trade-off has to be made. The product of the unambiguous velocity and range is given by (Doviak and Zrnić, 1993):

$$V_i^u \cdot R_i^u = \frac{c \, \lambda}{8} \tag{2}$$

where c is the speed of light. For a typical C-band ($\lambda = 5.3$ cm) radar, this product is roughly equal to 2000 km m s^{-1}. At a moderate range of 200 km, the unambiguous velocity is only 10 m s^{-1}. Velocities higher than the unambiguous one will be folded into the unambiguous interval (aliasing).

Dazhang et al. (1984) have proposed to extend the maximum unambiguous Doppler velocity by use of two alternating pulse repetition frequencies. From equation 1 it is clear that the use of different PRFs results in different unambiguous velocities. The folding of a measured velocity will, therefore, be different for the two pulse repetition frequencies. By combining the velocity measurements at the two different PRFs, the unambiguous velocity interval can be extended. Using a high and a low PRF with unambiguous velocities of V_h^u and V_l^u, respectively, the extended unambiguous velocity becomes (Dazhang et al., 1984):

$$V_{lh}^u = \frac{V_h^u \cdot V_l^u}{V_h^u - V_l^u} \tag{3}$$

It is evident from this equation that the unambiguous velocity interval is extended significantly when the high and low unambiguous velocities are close. It is common practice to choose the low and high PRFs such that the two unambiguous velocities are related in the following way:

$$\frac{V_h^u}{V_l^u} = \frac{\mathrm{PRF}_h}{\mathrm{PRF}_l} = \frac{N+1}{N} \tag{4}$$

where the integer N is the dual-PRF unfolding factor. By insertion of equation 4 into equation 3 it can be verified that N is indeed the factor by which the unambiguous velocity is extended with respect to V_h^u. With typical applications of the dual-PRF technique, an unfolding factor N of 2, 3, or 4 is used. It will be detailed below that for higher unfolding factors the quality of the measured velocities will be too poor.

A Doppler radar generally determines the radial velocity of the scatterers by autocorrelation of the received signal for subsequent send pulses. During pulse-pair processing the velocity is effectively deduced from the phase jump of the received signal between two subsequent pulses. The difference between the phase jump observed using the low PRF and that observed using the high PRF is employed by the dual-PRF technique to deduce the radial velocity. Because the velocity is directly related to the observed phase difference or jump, the dual-PRF velocity estimate can be expressed in terms of the original velocities only:

$$\tilde{V}_{lh} \;=\; (N+1)\tilde{V}_l - N\tilde{V}_h \tag{5}$$

where $\tilde{V}_l$ and $\tilde{V}_h$ are the observed velocities using the low and high PRF, respectively. When a dual-PRF velocity estimate falls outside of its unambiguous velocity interval as given by equation 3, it should be folded back into the fundamental interval by addition or subtraction of $2 \cdot V_{lh}^u$.

The dual-PRF velocity estimate is obtained by differencing of two phase measurements, and therefore its standard deviation will be amplified. Using equation 5 and assuming that the errors in the high and low PRF velocities are uncorrelated, the standard deviation of the dual-PRF velocity estimate becomes:

$$\sigma_{lh} \;=\; \sqrt{(N+1)^2\sigma_l^2 + N^2\sigma_h^2} \tag{6}$$

$$\simeq\; \bar{\sigma}\,\sqrt{(N+1)^2 + N^2} \tag{7}$$

where σ_l and σ_h are the standard deviations of the low and high PRF velocities, respectively. Usually these two standard deviations are roughly equal, and they can be replaced by their average $\bar{\sigma}$. In table 1 the calculated amplification of the standard deviation of the dual-PRF velocity with respect to the averaged original one is given for relevant unfolding factors. It is evident that the standard deviation of the dual-PRF velocity estimate increases rapidly with increasing unfolding factor.

In practice, the dual-PRF velocity estimate is not a suitable velocity estimator because of the large standard deviation (Sirmans et al., 1976; Dazhang et al., 1984; SIGMET, 1998). The dual-PRF velocity estimate is merely used to indicate to which Nyquist interval the original

Table 1: *Amplification of the standard deviation of the dual-PRF velocity estimate with respect to that of the original/dealiased velocity as a function of the unfolding factor* N.

N	2	3	4	5
$\sigma_{lh}/\bar{\sigma}$	3.6	5.0	6.4	7.8

(folded) velocity estimates belong. In this way, unfolded velocity estimates are obtained with the standard deviation of the original (folded) velocities. This two-step procedure introduces a type of errors in the velocity estimates that is distinctive for the dual-PRF retrieval technique. Occasionally, the deviation of the dual-PRF velocity estimate will be so large that the original folded velocity will be assigned to an incorrect Nyquist interval. This will give rise to clear outliers in the dual-PRF velocity data. In section 4 the origin and characteristics of these outliers will be discussed in more detail.

3 Available Doppler data

KNMI operates two identical C-band Doppler weather radars, one in De Bilt and one in Den Helder. In this study only data from the radar in De Bilt has been used. This radar is located at (52.10N,5.17E) and mounted at a height of 44 m above mean sea level. The Gematronik radar (Meteor AC360) has an antenna with a 4.2 m diameter and a beam width of about 1 degree. The send pulse of the radar is generated by a magnetron, and has a peak power of about 250 kW and a width of 0.5 μs (short pulse).

The returned signal is transferred to an analog receiver and subsequently digested by a Sigmet radar processor (RVP6). The radial velocity and spectral width are extracted from the received in-phase and quadrature phase components using pulse-pair processing. Prior to the pulse-pair processing, ground clutter has been removed from the signal by an infinite impulse response filter in the time domain. The data is averaged to 0.5 km and 1 degree in range and azimuth, respectively. The collection of averaged data points as a function of range at a certain azimuth is denoted a "ray". In dual-PRF mode, the velocity is obtained by combining data from the actual ray with that from the previous ray. Subsequently, the velocity data from the actual ray is unfolded using the dual-PRF velocity estimate. The dual-PRF unfolding is completely handled by the radar processor (SIGMET, 1998). The data acquisition and generation of products is performed using the Rainbow software package (Gematronik). In dual-PRF mode, the radar processor labels each ray with "high" or "low" according to the PRF used during acquisition. Unfortunately Rainbow does not transfer these labels yet, but a workaround will be presented later on.

The operational scanning scheme of the radar, which consists of a 4 elevation volume scan every 5 minutes and a 14 elevation volume scan every 15 minutes, still has some gaps. These gaps have been used to perform a dedicated Doppler scan which is repeated every 15 minutes. This scan is recorded at an elevation of 0.5 degrees and an azimuthal speed of 4 rpm. Using PRFs of 750 ($V_l^u = 10.0$ m s^{-1}) and 1000 Hz ($V_h^u = 13.3$ m s^{-1}), the extended unambiguous velocity interval of the dual-PRF data becomes $V_{lh}^u = 39.9$ m s^{-1}.

4 Analysis of dual-PRF data

To elucidate the error characteristics of dual-PRF velocity data, an analysis of measured velocity data has been performed. Figure 1 shows a typical example of unprojected dual-PRF velocity data. This azimuthal scan has been recorded during the passage of a warm front. The velocity data is presented in a so-called "B-scope display" or range-azimuth indicator. From a close

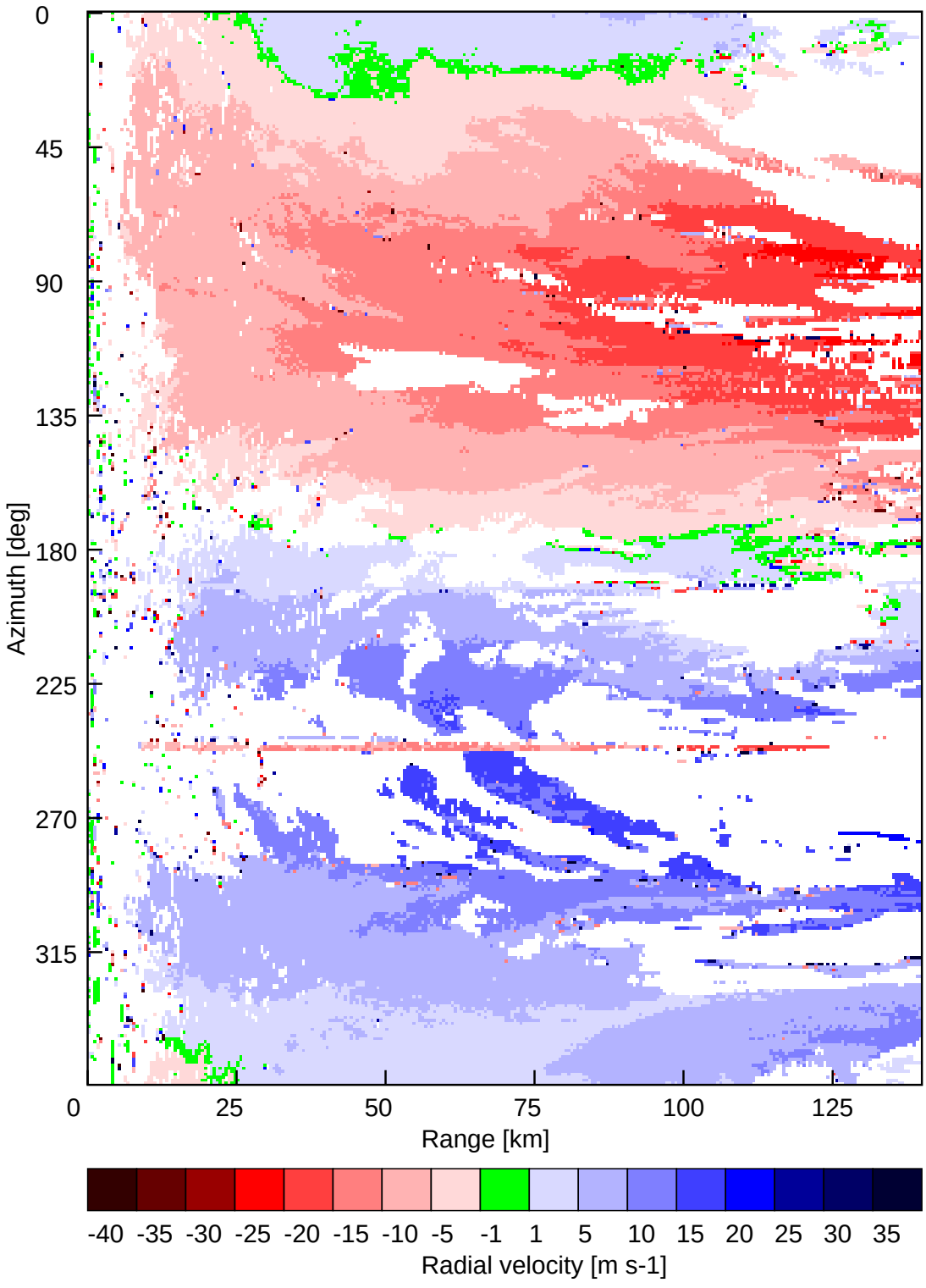

Figure 1: *B-scope display of raw dual-PRF velocity data from 1454 UTC 6 November 2001. The range from the radar and the azimuth are given on the horizontal and vertical axis, respectively. The azimuthal scan was recorded at an elevation of 0.5 degrees using PRFs of 750 and 1000 Hz.*

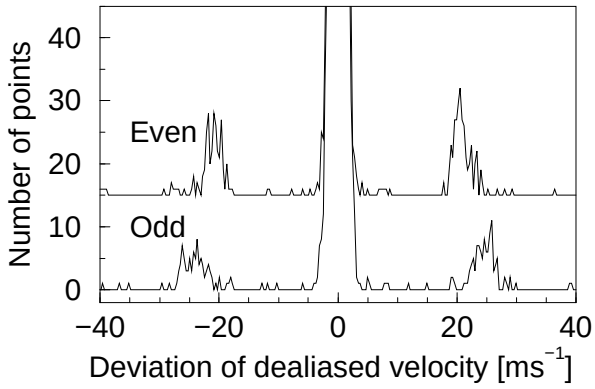

Figure 2: *Histogram of the deviations of each dealiased velocity from the local median velocity. This histogram has been compiled using the data of the azimuthal scan of Fig. 1. Separate histograms are shown for even and odd azimuths. The central peaks go up to a number of about 12,500 (off-scale).*

examination of Fig. 1 and other data, it appears that dual-PRF velocity data is typically contaminated by clutter, noise, and outliers. There is some sidelobe clutter present at short range in Fig. 1, but the most distinct clutter is caused by specular reflection of the radar beam from a building located at 246 degrees azimuth. Noise from incidental scatterers is predominantly visible at short range because the echoes from nearby targets are very strong. The presence of velocity outliers in large areas of high-quality data is characteristic for data obtained using the dual-PRF technique. These dual-PRF velocity outliers have been predicted and observed by others (Sirmans et al., 1976; Dazhang et al., 1984; Jorgensen et al., 2000; May and Joe, 2001). Large areas with falsely dealiased velocities, which are characteristic for single-PRF data, are not present in dual-PRF data provided that the maximum velocity is below the dual-PRF unambiguous velocity (Eq. 3).

A quantitative analysis has been performed to obtain detailed information on the quality and outliers of dual-PRF velocity data. For this, each velocity datapoint in an azimuthal scan is compared with the local median velocity. The local median velocity is calculated from the datapoint itself and the surrounding datapoints. An area measuring 5×3 points (range$\times$azimuth) is taken, and it is required that at least nine out of the fifteen datapoints contain valid data. The deviation of the datapoints from the local median values has been analyzed. In Fig. 2 histograms of the velocity deviations observed in the azimuthal scan of Fig. 1 are shown. For a reason that will become clear, velocity data from even and odd azimuths have been collected into different histograms. The histograms have been constructed using a bin size of 0.3 m s^{-1} which is equal to the resolution of the velocity data.

The central peaks of Fig. 2, containing the points with hardly any deviation from the local median velocity, go up to a number of about 12,500 (off-scale). The vast majority of the analyzed points obeys local continuity. The width of the central peaks is determined by the variance of the velocity data. A standard deviation of 0.50 and 0.49 m s^{-1} is obtained for the even and odd azimuths, respectively. The near equality of these standard deviations supports the assumption made in Eq. 7. Apart from the central peak, two distinct sideband peaks are evident in both histograms of Fig. 2. The sideband peaks correspond to the velocity outliers

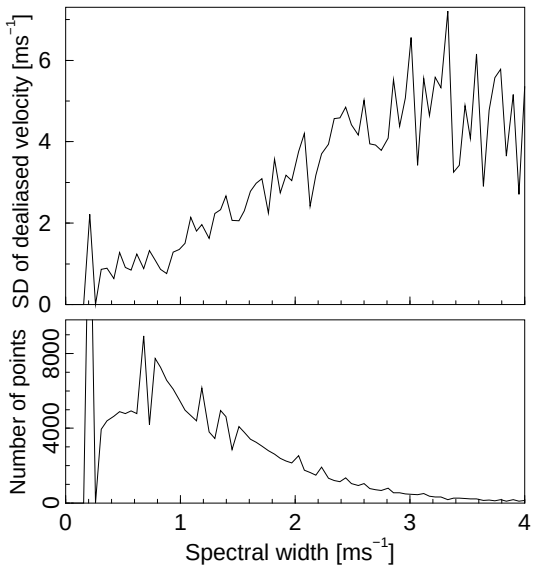

Figure 3: *In the upper frame of this figure the standard deviation of the dealiased velocities is shown as a function of the spectral width, and in the lower frame the number of datapoints per spectral width bin ($\simeq 0.1$ m s^{-1}) is shown. This figure has been put together using the velocity data from Fig. 1 and the corresponding spectral width data.*

which are characteristic for the dual-PRF technique. The number of points within the sidebands can be used to calculate the fraction of velocity outliers. The fraction of outliers is 9.1×10^{-3} and 7.3×10^{-3} for the even and odd azimuths, respectively. It is evident from Fig. 2 that the sidebands for even and odd azimuths are centered at different velocity deviations. The median deviation of the even azimuth sidebands is 20.9 m s^{-1} and that of the odd azimuth sidebands is 24.6 m s^{-1}. These velocity deviations roughly match the unambiguous intervals of the low PRF (20.0 m s^{-1}) and high PRF (26.6 m s^{-1}) measurements. It is, therefore, concluded in accordance with others (Dazhang et al., 1984; Jorgensen et al., 2000; May and Joe, 2001) that the velocity outliers in dual-PRF data are caused by dealiasing errors. In addition, the observed sideband positions of the even and odd azimuths can be used to assign the proper PRF (high or low) to each ray.

The standard deviation of a Doppler velocity measurement depends on the actual meteorological circumstances. By combining the dual-PRF velocity estimates with the spectral width data, this dependence can be demonstrated. For this, each velocity datapoint is again compared with the local median velocity. The standard deviation as a function of the spectral width is calculated by squaring the observed velocity deviations and summing them in different bins depending on the corresponding spectral width. The bin size is determined by the resolution of the available spectral width data and is equal to 0.1 m s^{-1}. By allowing a maximum velocity deviation of 11.6 m s^{-1}, equal to the average unambiguous velocity, possible outliers have been rejected. The upper frame of Fig. 3 shows the standard deviation as a function of spectral width as obtained from the azimuthal scan shown in Fig. 1 and the corresponding spectral width data. The number of datapoints per spectral width bin is shown in the lower frame of the figure. It is evident from Fig. 3 that the standard deviation depends strongly on the spectral width which is,

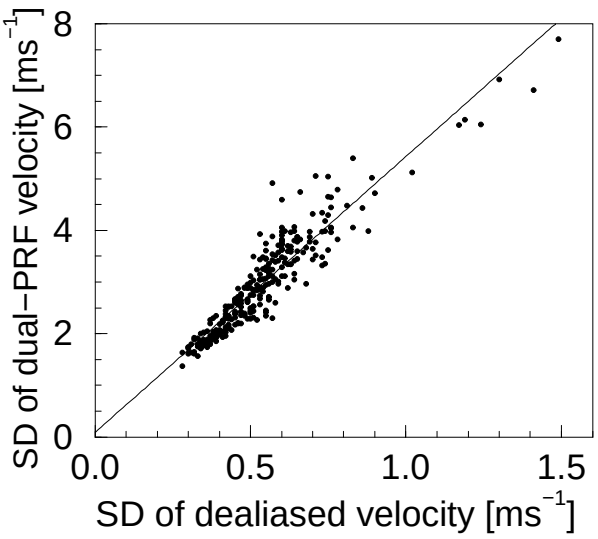

Figure 4: *Standard deviation of the dual-PRF velocity estimates as a function of the standard deviation of the original/dealiased velocities for about 300 different azimuthal scans. The method used for calculation of the standard deviations is described in the text. The scans have been selected by hourly scanning of real-time radar data for about a month and by taking only the scans containing more than 10,000 valid datapoints, i.e., about 10% of the datapoints in an azimuthal scan. The solid line with an intercept and slope of* 0.1 ± 0.1 *and* 5.3 ± 0.2*, respectively, is determined using linear regression.*

amongst others, affected by wind shear and turbulence (Doviak and Zrnić, 1993). The flattening of the curve for larger spectral widths ($>$3 m s^{-1}) is an artifact caused by a decreasing number of datapoints and limitations of the method for calculation of the standard deviation. The excessive number of datapoints (about 20,000) having a spectral width of 0.2 m s^{-1} seems unrealistic, but it is unexplained up to now. Although the overall trend of the standard deviation in Fig. 3 compares favorably to calculations by Doviak and Zrnić (1993), a quantitative comparison is hampered by lack of information on, for instance, the signal-to-noise ratio.

Because the dual-PRF dealiasing is completely handled by the radar processor, data from the intermediate step, i.e., the dual-PRF velocity estimates, are not available for further analysis. The dual-PRF velocity estimates can, however, be reconstructed to a large extent from the dealiased data. For this, it is crucial that for each ray is known which PRF (high or low) has been used during acquisition. When this information is not available, as in our case, it has to be deduced from the outlier analysis as presented in Fig. 2. The first step in the reconstruction is to fold the dealiased velocities back to their original fundamental Nyquist interval by adding or subtracting a multiple of $2V_l^u$ or $2V_h^u$ (depending on PRF). Subsequently, the dual-PRF velocity estimate can be calculated for each valid datapoint using Eq. 5 when valid data is present in the same rangebin of the previous ray as well. Using the method described previously, the standard deviation of the reconstructed dual-PRF velocity estimates can be calculated. In Figure 4 the standard deviation of the reconstructed dual-PRF velocities is plotted as a function of the standard deviation of the corresponding dealiased velocities for about 300 different azimuthal scans. The scans have been selected by hourly scanning of real-time radar data for about a

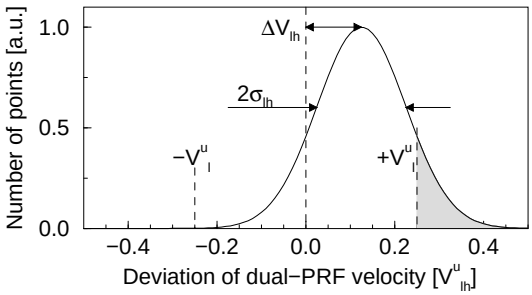

Figure 5: *Scheme illustrating the origin of the dealiasing errors in velocity data obtained using the dual-PRF technique. The distribution of deviations of the dual-PRF velocity estimates is depicted. The parameters influencing this distribution, i.e., standard deviation and bias, are indicated. The unambiguous velocity interval of the low-PRF measurement for $N = 3$ unfolding has been indicated in the figure as well. The fraction of incorrectly dealiased datapoints is marked by the shaded area.*

month and by taking only the scans containing more than 10,000 valid datapoints, i.e., about 10% of the datapoints in an azimuthal scan. A high correlation between the standard deviation of the dual-PRF velocities and that of the dealiased velocities is evident from Fig. 4. The line determined using linear regression is shown in the figure as well. The resulting intercept and slope are 0.1 ± 0.1 and 5.3 ± 0.2, respectively. Thus the standard deviation is about five times as large as that of the dealiased/original velocities which is in almost perfect agreement with the theoretical ratio for $N = 3$ unfolding (see Eq. 7 and Table 1).

The large standard deviation of the dual-PRF velocity estimate is together with possible azimuthal shear of the radial wind the main cause of dealiasing errors (outliers) in dual-PRF velocity data (Dazhang et al., 1984; May, 2001). The origin of the dealiasing errors has been depicted schematically in Figure 5. On the horizontal axis the deviation of the dual-PRF velocity estimate relative to its unambiguous value is given. The Gaussian curve represents the distribution of possible deviations of the dual-PRF velocities as implied by its standard deviation (σ_{lh}). The dual-PRF technique employing data of the current and previous ray neglects azimuthal shear of the radial wind, i.e., differences of true radial velocities in both rays. By insertion of a velocity difference in Eq. 5, the bias of the dual-PRF velocity estimate due to wind shear is obtained:

$$\Delta\tilde{V}_{lh}(\Delta S) = \begin{cases} -N\Delta S & \text{when PRF is low} \\ (N+1)\Delta S & \text{when PRF is high} \end{cases} \tag{8}$$

where ΔS is the azimuthal shear of the radial wind component. The bias, which has been indicated in Fig. 5, gets more pronounced for higher unfolding factors. The unambiguous velocity interval of the low PRF measurement for $N = 3$ unfolding has been indicated in the figure as well. When the dual-PRF velocity estimate is deviating more than the unambiguous velocity, the original velocity is assigned to an incorrect Nyquist interval. The fraction of incorrectly dealiased datapoints η, which is marked by the shaded area in Fig. 5, can be calculated using:

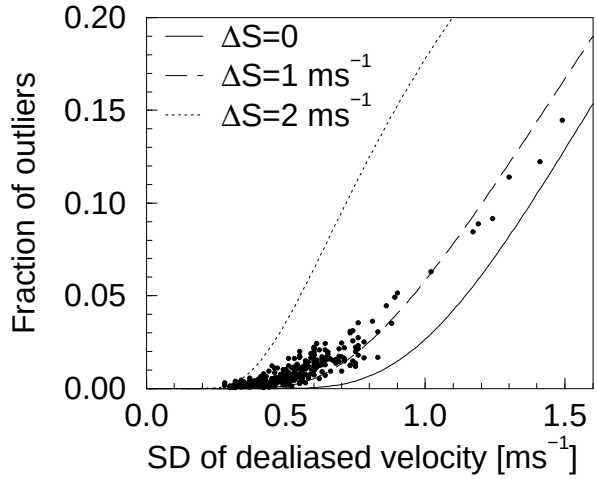

Figure 6: *Fraction of dealiasing errors as a function of the standard deviation of the original/dealiased velocities. About 300 different azimuthal scans (same scans as used in Fig. 4) have been used to compile this figure. In addition, three theoretical curves for azimuthal wind shears of 0, 1, and 2 m s^{-1} are shown.*

$$\eta_i = \frac{1}{2}\left[\text{erfc}\left(\frac{V_i^u - \Delta\tilde{V}_{lh}}{\sqrt{2}\sigma_{lh}}\right) + \text{erfc}\left(\frac{V_i^u + \Delta\tilde{V}_{lh}}{\sqrt{2}\sigma_{lh}}\right)\right] \quad (9)$$

$$\eta = \frac{1}{2}\left[\eta_l + \eta_h\right] \quad (10)$$

where erfc(x) is the complementary error function (Press et al., 1992). This equation describes the effect of both standard deviation and wind shear on the fraction of dealiasing errors in dual-PRF velocity data.

The fraction of velocity outliers and the standard deviation of the dealiased velocities can be determined from a dual-PRF Doppler azimuthal scan using the method described previously (see Fig. 2). In figure 6 the fraction of outliers is plotted as a function of the standard deviation of the dealiased velocities for about 300 different scans (same scans as used in Fig. 4). In addition, the theoretical dependence as implied by Eq. 10 is plotted for three different azimuthal shears of the radial wind. The standard deviation of the original/dealiased velocities has been converted to that of the dual-PRF velocity estimates using the multiplication factor given by Table 1. The solid curve representing the theoretical fraction of outliers without any wind shear neatly sets the lower boundary for the experimental data. The majority of the experimental datapoints in Fig. 6 is grouped around the theoretical curve for an azimuthal shear of 1 m s^{-1}. For a typical standard deviation of 0.5 m s^{-1}, the fraction of dealiasing errors is on the order of 0.01. For higher unfolding factors, the number of dealiasing errors will increase dramatically due to the increase of the standard deviation of the dual-PRF velocity estimate. Equation 10 can also be utilized to quantitatively investigate the effect of changing the unfolding factor from $N = 3$ to, for instance, $N = 4$. For a typical standard deviation of $\bar{\sigma} = 0.5$ m s^{-1} and a wind shear of $\Delta S = 1.5$ m s^{-1}, the fraction of outliers increases from 0.008 to 0.05 upon this slight increase

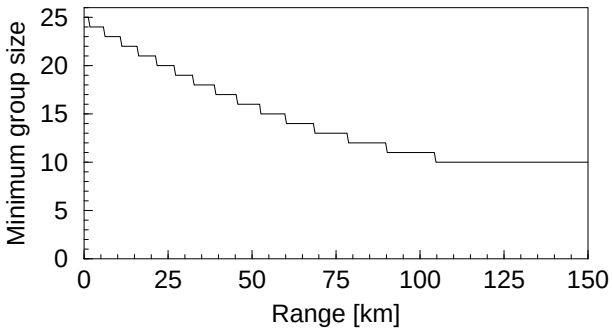

Figure 7: *Minimum required number of datapoints per group as a function of the maximum range of the group. Groups of connected datapoints with less points will be removed from the raw data. This parabolic curve is characterized by the minimum group size at zero range (25) and that at maximum range (10), where the parabola has its minimum.*

of the unfolding factor. It will be detailed below that (a limited amount of) dealiasing errors can be corrected in a reliable way.

5 Correction of dual-PRF data

From the preceding it is evident that radial velocity data obtained using the dual-PRF technique cannot be fed as such to feature detection algorithms or a dual-Doppler wind field analysis. In this section a three-step post-processing algorithm is proposed which enhances the quality of the dual-PRF velocity data significantly. This algorithm is intended for real-time operational use and will be implemented at KNMI in the near future. It will be shown that the quality of the dual-PRF velocity data thus becomes high enough to enable all kinds of further use. The post-processing algorithm essentially consists of the following steps:

1. Removal of clutter and noise. The dual-PRF velocity data is filtered based on the size and the clutter fraction of groups of connected datapoints.

2. Global dealiasing. Dealiasing of radial velocities that fall outside of the extended unambiguous velocity interval. This step is primarily performed to ensure robustness of the algorithm, because the extended unambiguous velocity interval is usually large enough.

3. Local dealiasing. Using the known error characteristics of the dual-PRF data, velocity outliers are corrected in an efficient and responsible way.

It should be noted that these steps have to be performed on the data in the listed order. All steps of the algorithm will be described in more detail below.

During the first step, clutter and noise are removed from the dual-PRF data. As a start, clutter from nearby buildings or other targets is removed by deleting the affected rays of the azimuthal scan. Subsequently, a filter based on the size and clutter fraction of groups of connected datapoints is applied. For this, groups of connected (valid) datapoints are labeled using an efficient algorithm described by Gonzalez and Woods (1992) and a ready algorithm for sorting labels into equivalent classes (Press et al., 1992). The labeling algorithm only looks for

connections via the four closest neighbors of each datapoint. The periodical boundary of the polar radar data in azimuthal direction is treated properly. Then, the number of datapoints and 'zero velocity' points (V$<$1.5 m s^{-1}) per group of connected datapoints are counted. Groups consisting of less than a certain minimum number of datapoints are removed entirely from the azimuthal scan. In Figure 7 the minimum number of datapoints per group is plotted as a function of the maximum range of the group. The minimum group size is 25 at zero range, and it gradually decreases to 10 at maximum range. The rationale behind this range dependence is the decrease of the volume represented by each datapoint for a shortening range. Up to a range of about 25 km, groups containing more 'zero velocity' points than other points are removed entirely from the azimuthal scan as well. Via this "group size" filtering, noise from incidental scatterers at short ranges and persistent clutter due to sidelobes are removed effectively without affecting the signal at long ranges. After filtering of a scan, the minimum size of groups of connected datapoints is known, and this will be of advantage during the third step of the algorithm. In the remaining, all valid datapoints will be preserved and only be corrected when needed.

The global dealiasing, which is the second step, usually has no effect on the data, but is designed to restore large scale dealiasing errors. Velocities outside of the extended unambiguous interval, which is 40 m s^{-1} in our case, cannot be dealiased correctly by the dual-PRF technique. These dealiasing errors will result, just as for single-PRF velocity data (Doviak and Zrnić, 1993; Eilts and Smith, 1990; Jing and Wiener, 1993), in long boundaries of velocity discontinuities and large areas with incorrect velocity values. For dual-PRF data, however, this kind of dealiasing errors hardly ever occurs because of the extended unambiguous velocity interval. Numerous methods for (global) dealiasing of single-PRF data that in principle can also be applied to dual-PRF data have been developed (Ray and Ziegler, 1977; Merritt, 1984; Desrochers, 1989; Eilts and Smith, 1990; Jing and Wiener, 1993). Most methods rely heavily on local continuity of the wind field and use a reference wind profile (Eilts and Smith, 1990) or a wind model (Merritt, 1984) for dealiasing of isolated areas. Taking into account the large unambiguous interval of the dual-PRF data, a rather straightforward method based on a reference wind profile is adopted. The wind profile is used to determine the proper Nyquist interval for each datapoint (Hennington, 1981), and the velocities are dealiased by adding or subtracting $2 \cdot V_{lh}^{u}$ ($\simeq 80$ m s^{-1}). An upper-air sounding or a model profile can be used as the reference profile, but the use of a radar VAD (Browning and Wexler, 1968) or VVP (Waldteufel and Corbin, 1979) profile is preferred. These radar wind profiles are based on a linear wind model and are by definition available at the radar site. Aliasing errors are generally no problem in these profiles, because of differences in measurement strategy and corrections made by the profile algorithms. This step is implemented as a safety because the third step cannot handle large scale dealiasing errors.

During the third and final step, local dealiasing errors (outliers) are corrected using the known error characteristics of dual-PRF data. It has been detailed in section 4 that outliers can be identified by their deviation from the local median velocity. The calculation of the local median velocity is based on at least nine valid datapoints. In first instance the nine datapoints are sought in the 3×3 square centered at the datapoint. When not enough valid datapoints are present in this square, the square is enlarged step by step until the required number of points is collected. The "adaptive" local median velocity can be determined for each datapoint, since the minimum number of connected points per group is known from the "group size" filtering of the first step. Datapoints deviating more than the unambiguous velocity from the local median velocity are considered as outliers. For both the detection and correction of the outliers, it

is crucial that the PRF (high or low) and thus the unambiguous velocity is known for each ray. This information can be obtained from the histogram analysis presented in Fig. 2, but it should be extracted from the radar processor to ensure operational robustness. The deviation of the outliers from the local median velocity is minimized by adding or subtracting multiples of twice the appropriate unambiguous velocity. By correcting the outliers in this way, the spatial resolution of the velocity data is retained and no smoothing of any kind is applied. In addition, this correction method is very efficient because the local median velocity remains representative for up to four nearby outliers (out of nine). Several passes of the local dealiasing algorithm may be advantageous when the local concentration of outliers is high, for instance in areas with a high wind shear or a large spectral width.

Preliminary results on the performance of the three-step post-processing algorithm have been obtained. The algorithm has been applied to the 300 azimuthal scans already used in Figs. 4 and 6. During the processing of the scans, the average fraction of outliers and the percentage of high-quality scans have been monitored. Azimuthal scans with a fraction of outliers (η) smaller than 0.001 are defined to be of "high quality" in this study. The results for the raw scans, the "group size" filtered scans, and the corrected scans after one, two, and three pass(es) of local dealiasing algorithm are listed in Table 2. The averaged outlier fraction of the untreated scans is roughly 0.01 (see also Fig. 6) and the percentage of high-quality scans is only 3.5%. On average, about 7% of the datapoints is removed by group size filtering of the azimuthal scans. The first pass of the local dealiasing algorithm decreases the average fraction of outliers by almost a factor of 30 and increases the percentage of high-quality scans to roughly 90%. After the second pass, the percentage of high-quality scans is already approaching 100%. So high-quality velocity data is usually obtained by application of the post-processing algorithm with only a single pass of the local dealiasing algorithm.

6 Conclusions

Fields of radial velocity data obtained using the dual-PRF technique have been analyzed quantitatively. The standard deviation of the velocity estimates and the fraction of dealiasing errors (outliers) are extracted. In addition, the positions of the outlier sidebands as observed for rays with even and odd azimuths can be used to assign the proper PRF to each ray. It is shown experimentally that the standard deviation of the velocity estimates depends on the spectral width

Table 2: *Results of the application of the three-step post-processing algorithm on about 300 azimuthal scans (same scans as used in Fig. 4 and Fig. 6). The average fraction of outliers ($\bar{\eta}$) and the percentage of high-quality scans, i.e., with a fraction of outliers $\eta < 0.001$, are considered. The results for the raw scans, the "group size" filtered scans, and the corrected scans after one, two, and three pass(es) of local dealiasing algorithm are listed.*

	raw	filter	1st pass	2nd pass	3rd pass
$\bar{\eta}$	0.011	0.010	3.9×10^{-4}	1.1×10^{-4}	6.3×10^{-5}
$\eta \leq 0.001$	3.5%	4.2%	89.5%	99.3%	99.7%

and thus on the meteorological circumstances. A simple model has been employed to describe the dependence of the fraction of dealiasing errors on the standard deviation of the velocity estimates and the azimuthal shear of the radial wind. Quantitative agreement between the observed and modeled fraction of dealiasing errors as a function of the standard deviation is found.

A three-step post-processing algorithm for enhancing the quality and thus the employability of dual-PRF velocity data has been developed. The post-processing algorithm, which removes noise and corrects dealiasing errors, is intended for operational use. The spatial resolution of the velocity data is retained, however, because no smoothing is performed. Preliminary results on the performance of the algorithm have been obtained by processing of about 300 azimuthal scans. It is found that high-quality dual-PRF velocity data, i.e., scans with a fraction of outliers smaller than 0.001, are produced routinely using the three-step algorithm. The majority of the azimuthal scans (90%) is upgraded to high-quality in a single pass of the local dealiasing algorithm (third step of algorithm) while for the remaining ones only two or three passes are needed. In conclusion, the post-processing algorithm is very efficient and produces dual-PRF velocity data of high quality. Bird migration and ground clutter may still cause problems in the (processed) dual-PRF velocity data, just as they would in single-PRF data. The post-processing algorithm for dual-PRF data will be implemented at KNMI, and this will enable further development of Doppler radar applications, like detection of wind shear, dual-Doppler wind fields, and assimilation into NWP models.

Acknowledgments

Herman Wessels and Sylvia Barlag are gratefully acknowledged for their support and careful reading of the manuscript.

REFERENCES

Bergen, W. R. and S. C. Albers: 1988, Two- and Three-Dimensional De-aliasing of Doppler Radar Velocities. *J. Atmos. Ocean. Technol.*, **5**, 305–319.

Browning, K. A. and R. Wexler: 1968, The Determination of Kinematic Properties of a Wind Field using Doppler Radar. *J. Appl. Meteor.*, **7**, 105–113.

Chong, M., J.-F. Georgis, O. Bousquet, S. R. Brodzik, C. Burghart, S. Cosma, U. Germann, V. Gouget, R. A. Houze, Jr., C. N. James, S. Prieur, R. Rotunno, F. Roux, J. Vivekanandan, and Z.-X. Zeng: 2000, Real-Time Wind Synthesis from Doppler Radar Observations during the Mesoscale Alpine Programme. *Bull. Amer. Meteor. Soc.*, **81**, 2953–2962.

Collins, W. G.: 2001, The Quality Control of Velocity Azimuth Display (VAD) Winds at the National Centers for Environmental Prediction. *11th Symposium on Meteorological Observations and Instrumentation*, Albuquerque, NM, AMS, 317–320.

Dazhang, T., S. G. Geotis, R. E. Passarelli Jr., A. L. Hansen, and C. L. Frush: 1984, Evaluation of an Alternating-PRF Method for Extending the Range of Unambiguous Doppler Velocity. *22nd conference on Radar Meteorology*, Zürich, Switzerland, Amer. Meteor. Soc., 523–527.

Desrochers, P. R.: 1989, A Reliable Method for Real-Time Velocity Unfolding. *24th conference on Radar meteorology*, Tallahassee, FL, Amer. Meteor. Soc., 415–418.

Doviak, R. J. and D. S. Zrnić: 1993, *Doppler Radar and Weather Observations*. Academic Press, second edition, 562 pp.

Eilts, M. D. and S. D. Smith: 1990, Efficient Dealiasing of Doppler Velocities Using Local Environment Constraints. *J. Atmos. Ocean. Technol.*, **7**, 118–128.

Gonzalez, R. C. and R. E. Woods: 1992, *Digital Image Processing*. Addison-Wesley Publishing Company, first edition, 716 pp.

Hennington, L.: 1981, Reducing the Effects of Doppler Radar Ambiguities. *J. Appl. Meteor.*, **20**, 1543–1546.

Hondl, K. D. and M. D. Eilts: 1993, Evaluation of Doppler Velocity Dealiasing Techniques for Low-Nyquist Velocity Data. *26th conference on Radar Meteorology*, Norman, OK, Amer. Meteor. Soc., 59–61.

Jing, Z. and G. Wiener: 1993, Two-Dimensional Dealiasing of Doppler Velocities. *J. Atmos. Ocean. Technol.*, **10**, 798–808.

Jorgensen, D. P., T. R. Shepherd, and A. S. Goldstein: 2000, A Dual-Pulse Repetition Frequency Scheme for Mitigating Velocity Ambiguities of the NOAA P-3 Airborne Doppler Radar. *J. Atmos. Ocean. Technol.*, **17**, 585–594.

Lindskog, M., H. Järvinen, and D. B. Michelson: 2000, Assimilation of Radar Radial Wind in the HIRLAM 3D-Var. *Phys. Chem. Earth (B)*, **25**, 1243–1250.

May, P. T.: 2001, Mesocyclone and Microburst Signature Distortion with Dual PRT Radars. *J. Atmos. Ocean. Technol.*, **18**, 1229–1233.

May, P. T. and P. Joe: 2001, The Production of High Quality Doppler Velocity Fields for Dual PRT Weather Radar. *30th conference on Radar Meteorology*, Münich, Germany, Amer. Meteor. Soc., 286–288.

Meischner, P., C. Collier, A. Illingworth, J. Joss, and W. Randeu: 1997, Advanced Weather Radar Systems in Europe: The COST 75 Action. *Bull. Amer. Meteor. Soc.*, **78**, 1411–1430.

Merritt, M. W.: 1984, Automatic Velocity De-aliasing for Real-Time Applications. *22nd conference on Radar meteorology*, Zürich, Switzerland, Amer. Meteor. Soc., 528–533.

Press, W. H., S. A. Teukolsky, W. T. Vetterling, and B. P. Flannery: 1992, *Numerical Recipes in C: the Art of Scientific Computing*. Cambridge University Press, second edition, 994 pp.

Ray, P. S. and C. Ziegler: 1977, De-aliasing First-Moment Doppler Estimates. *J. Appl. Meteor.*, **16**, 563–564.

Sachidananda, M. and D. S. Zrnić: 2000, Clutter Filtering and Spectral Moment Estimation for Doppler Weather Radars Using Staggered Pulse Repetition Time (PRT). *J. Atmos. Ocean. Technol.*, **17**, 323–331.

Serafin, R. J. and J. W. Wilson: 2000, Operational Weather Radar in the United States: Progress and Opportunity. *Bull. Amer. Meteor. Soc.*, **81**, 501–518.

SIGMET: 1998, RVP6 Doppler Signal Processor User's Manual.

Sirmans, D., D. Zrnić, and B. Bumgarner: 1976, Extension of Maximum Unambiguous Doppler Velocity by Use of Ywo Sampling Rates. *17th conference on Radar Meteorology*, Seattle, WA, Amer. Meteor. Soc., 23–28.

Waldteufel, P. and H. Corbin: 1979, On the Analysis of Single-Doppler Radar Data. *J. Appl. Meteor.*, **18**, 532–542.